Effects of an electromagnetic field on intracellular calcium oscillations in a cell with external noise*

Duan Wei-Long(段卫龙)[a)], Yang Lin-Jing(杨林静)[b)], and Mei Dong-Cheng(梅冬成)[a)†]

[a)] *Department of Physics, Yunnan University, Kunming* 650091, *China*

[b)] *College of Chinese Medicine, Yunnan University of Traditional Chinese Medicine, Kunming* 650031, *China*

(Received 6 September 2010; revised manuscript received 28 September 2010)

Intracellular calcium ion concentration oscillation in a cell subjected to external noise and irradiated by an electromagnetic field is considered. The effects of the intensity E_0, the polar angle θ and the frequency ω of the external electric field on steady-state probability distribution and the mean Ca^{2+} concentration, respectively, are investigated by a numerical calculation method. The results indicate that (i) variation of ω cannot affect the intracellular calcium oscillation; (ii) the steady-state probability distribution presents a meaningful modification due to the variations of E_0 and θ, while variation of θ does not affect the steady-state probability distribution under the condition of a small E_0, and E_0 cannot affect the steady-state probability distribution either when $\theta = \pi/2$; (iii) the mean Ca^{2+} concentration increases as E_0 increases when $\theta < \pi/2$ and, as θ increases, it first increases and then decreases. However, it does not vary with E_0 increasing when $\theta = \pi/2$, but it increases with θ increasing when E_0 is small.

Keywords: fluctuation phenomena，interactions of biosystems with radiations

PACS: 05.40.–a, 87.50.–a **DOI:** 10.1088/1674-1056/20/3/030503

1. Introduction

The calcium ion Ca^{2+} is one of the most versatile and universal signaling agents in biological processes such as fertilization, cell proliferation, muscle contraction and synaptic plasticity and apoptosis, and studies have revealed that Ca^{2+} oscillation plays an important role in some of these processes.[1] Many different models have been developed to describe Ca^{2+} oscillation.[2−5] Among them there is a model in which a cell is supposed to be comprised of a cell membrane, cytosol and Ca^{2+} store.[2] There is a layer membrane between the cytosol and the Ca^{2+} store. The Ca^{2+} is removed from the cytosol in two principal ways: one is to pump it out of a cell and the other is to sequester it into internal Ca^{2+} store (ICS). Since the Ca^{2+} concentration in the cytosol is much lower than that in the extracellular medium or inside the ICS, Ca^{2+} influx also occurs via two main pathways: inflowing from the extracellular medium through Ca^{2+} channels into the surface membrane and releasing from the ICS. The models for cytosol calcium oscillations using xenopus oocytes,[6] for receptor-controlled cytosol calcium oscillations[7] and for calcium oscillations due to negative feedback in olfactory cilia[8] have been proposed and studied. Additionally, the models for intercellular calcium oscillations in hepatocytes,[9] astrocytes[10] and the lamprey[11] have also been obtained. A simple one-pool model has been put forward,[12] with which hormone-induced calcium oscillations in liver cells has been explained.[13] Tesarik and Sousa[14] used a two-store model to explain the mechanism of calcium oscillations in human oocytes. The crosstalk between cellular morphology and calcium oscillation patterns has been studied using a stochastic computer model.[15] Berridge[16] investigated the relationship between latency and period for 5-hydroxytryptamine-induced membrane responses in the salivary gland of Calliphora, and Gapeyev and Chemeris[17] researched the influence of modulated electromagnetic radiation of extremely high frequencies on nonlinear modification of neutrophil calcium homeostasis. Moreover, the internal signal stochastic resonance,[18−20] internal noise affecting coherence resonance induced by external noise,[21] sustaining synchronized oscillation,[22] internal noise enhancing detection[23] and transduction[24] of a hormonal signal in a calcium oscillation system have also been studied. More recently, hysteresis and bistability in a realistic cell model for calcium oscillation and action potential firing were studied.[25] However, to our knowledge, the effect of an external electromagnetic field on intracellular Ca^{2+} oscillation in

*Project supported by the National Natural Science Foundation of China (Grant No. 10865006) and the Science Foundation of Yunnan University, China (Grant No. 2009A001Z).

†Corresponding author. E-mail: meidch@ynu.edu.cn

© 2011 Chinese Physical Society and IOP Publishing Ltd

a cell subjected to external noise has not yet been considered. Therefore, the influence of the external electromagnetic field surrounding a cell on intracellular calcium oscillation needs to be investigated.

In this paper, we study the variations of the Ca^{2+} concentration in cytosol X and in the ICS Y under the influence of an external electromagnetic field $\boldsymbol{E}$ using the sketch of a spherical cell with an ICS in the centre. The remainder of the present paper is organized as follows. In Section 2, we use the model proposed in Ref. [2] to compute the transmembrane potential of the ICS and then use the Boltzman density distribution law to express the relation between X and Y. The Langevin equation (LE) and corresponding Fokker–Planck equation (FPE) of the system are derived. Based on them, the steady-state probability distribution (SPD) $P_{\rm S}(X)$ of cytosol Ca^{2+} concentration and the SPD $P_{\rm S}(Y)$'s of ICS Ca^{2+} concentration, steady-state mean cytosol Ca^{2+} concentration $< X >$ and ICS Ca^{2+} concentration $< Y >$ are obtained. In Section 3, we analyse the influence of the intensity, the polar angle and the frequency of the external electric field on $P_{\rm S}(X)$, $P_{\rm S}(Y)$, $< X >$ and $< Y >$ by the numerical computations. A brief conclusion is presented in Section 4.

2. Steady-state probability distribution and mean Ca^{2+} concentration

In the present work, we use a simple model used in Ref. [2], which states that there is an ICS in the centre of the cell and the uptake and release of Ca^{2+} ions from the ICS is controlled by cytosol Ca^{2+} concentration. The Ca^{2+}-induced Ca^{2+} release can occur by a positive feedback from the ICS. Two variables, i.e., cytosol Ca^{2+} concentration X and the Ca^{2+} concentration Y of the ICS, are used in the model, satisfying the following equations:[2]

$$\frac{{\rm d}X}{{\rm d}t} = V_0 + \beta V + k_{\rm f}Y - kX - V_1(X,Y) + V_2(X,Y), \quad (1)$$

$$\frac{{\rm d}Y}{{\rm d}t} = V_1(X,Y) - V_2(X,Y) - k_{\rm f}Y, \quad (2)$$

where V_0 is a steady flow of Ca^{2+} to the cytosol; V is the maximum rate of stimulus-induced influx of Ca^{2+} from the extracellular medium; β is a control parameter representing the degree of stimulation of the extracellular medium, which varies between 0 and 1.[26] In the study of the phenomenon of the explicit internal signal stochastic resonance in Ref. [20], the external noise $\xi(t)$ is added to the controlling parameter β. For simplicity, we assume β to be

$$\beta = \beta_0 + D\xi({\rm t}), \quad (3)$$

in which β_0 is a constant of β in a period-2 oscillatory state; D is the noise intensity that represents the degree of the effect of the environment noise acting on the system; $\xi(t)$ is a Gaussian white noise with a zero mean value ($< \xi(t) >= 0$) and unit variance ($< \xi(t)\xi(t+\tau) >= \delta(\tau)$), which is generated by a Band-limited white noise generator. In the present paper, we take a appropriate noise intensity $D = 0.05$ because we are mainly researching the effect of the electromagnetic field on intracellular calcium oscillation. We set $V_0 = V = 2$ μM/s and $\beta_0 = 0.772$. Let $-kX$ denote the uptake from cytosol, $V_1(X,Y)$ represent the active uptake of Ca^{2+} from the cytosol to the ICS, $V_2(X,Y)$ refer to the active release of Ca^{2+} from the ICS to the cytosol, and $k_{\rm f}Y$ describe a diffusion flow of Ca^{2+} from the ICS to the cytosol, then the active flows will be assumed to be in the following forms:[2]

$$V_1(X,Y) = \frac{V_{1\rm m}X^2}{k_2^2 + X^2}, \quad (4)$$

$$V_2(X,Y) = \frac{V_{2\rm m}X^4Y^2}{(k_{\rm a}^4 + X^4)(k_{\rm r}^2 + Y^2)}. \quad (5)$$

The parameters are set to be $V_0 = 2$ μM/s, $k_{\rm f} = 2 \times 10^{-5}$/s, $k = 1 \times 10^3$/s, $V_{1\rm m} = 65$ μM/s, $V_{2\rm m} = 500$ μM/s, $k_2 = 1$ μM, $k_{\rm a} = 0.9$ μM, and $k_{\rm r} = 2$ μM (1 M = 1 mol/dm^3) in the present work.

According to the Boltzman density distribution law, the relationship between the cytosol Ca^{2+} concentration X and the ICS Ca^{2+} concentration Y can be expressed as[27]

$$Y = X \exp\left(\frac{nU}{\gamma U_{\rm T}}\right), \quad (6)$$

in which, U is the transmembrane potential of the ICS membrane, $n = 2$ is the quantivalency of Ca^{2+}, $U_{\rm T} = k_{\rm B}T/e$ is the thermodynamic potential expressed in volts and γ is a revised factor brought forth due to the influence of the external potential on geometry shape and electric particles generating and combining in the lipid bilayer, and $\gamma U_{\rm T} = 5.2$ mV as given in Ref. [27]. We set $\alpha = n/\gamma U_{\rm T} = 0.38$ mV^{-1}. Here, we employ the scheme of a spherical cell irradiated by a electromagnetic field $\boldsymbol{E} = E_0\,{\rm e}^{{\rm i}\omega t}\boldsymbol{e}_x$ in the x direction as illustrated in Fig. 1, in which the parameters are the same as those in Ref. [28].

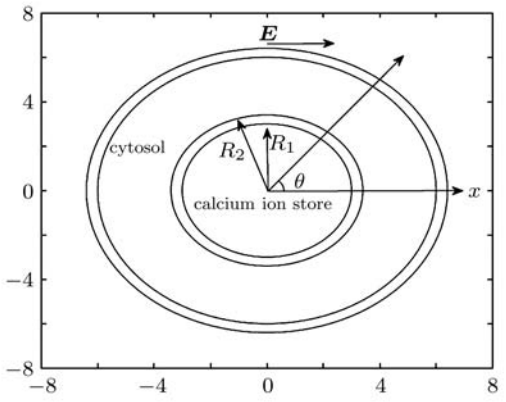


Fig. 1. Schematic of a spherical cell with an ICS in the centre.

Furthermore, the electric field around the ICS can be considered as being an uniform electric field in the x-direction because the volume of the ICS is very much smaller than that of the cell, thus, the electromagnetic field around the ICS reads $\boldsymbol{E} = lE_0\,\mathrm{e}^{\mathrm{i}\omega t}\boldsymbol{e}_x$ based on refraction law, where l is constant. In the present paper, the value of l has no effect on our research, therefore, we still take electromagnetic field around the ICS as $\boldsymbol{E} = E_0\,\mathrm{e}^{\mathrm{i}\omega t}\boldsymbol{e}_x$. Accordingly, $\boldsymbol{E}$ will lead to an additional potential in the ICS membrane, and U can be expressed as[27]

$$U = U_0 + U_{\mathrm{m}}\cos(\omega t), \tag{7}$$

where U_0 is the transmembrane potential of the ICS without the external electromagnetic field $\boldsymbol{E}$, and U_{m} is the peak of transmembrane potential induced by the electromagnetic field in the ICS. Generally speaking, we have $U_0 > U_{\mathrm{m}}$. Substituting Eq. (7) into Eq. (6) and performing a Taylor expansion at $U = U_0$, one can obtain[27]

$$Y = X\,\mathrm{e}^{\alpha U_0}\left[1 + \frac{\alpha^2 U_{\mathrm{m}}^2}{4} + \alpha U_{\mathrm{m}}\cos(\omega t) + \frac{\alpha^2 U_{\mathrm{m}}^2}{4}\cos(2\omega t) + \ldots\right] \approx X\,\mathrm{e}^{\alpha U_0}\left(1 + \frac{\alpha^2 U_{\mathrm{m}}^2}{4}\right). \tag{8}$$

To obtain the expression of U_{m}, firstly, we derive the potential distributions of inside and outside the ICS. The potential distribution enclosed by, within and surrounding a single membrane particle in suspension with $\boldsymbol{E} = E_0\,\mathrm{e}^{\mathrm{i}\omega t}\boldsymbol{e}_x$ in the x direction was derived respectively as[29]

$$\Phi_1(r,\theta) = a(\omega) r\cos(\theta), \tag{9}$$

$$\Phi_2(r,\theta) = \left[b(\omega) + \frac{c(\omega)}{r^3}\right] r\cos(\theta), \tag{10}$$

$$\Phi_3(r,\theta) = \left[\frac{d(\omega)}{r^3} - E_0\right] r\cos(\theta), \tag{11}$$

where $a(\omega)$, $b(\omega)$, $c(\omega)$ and $d(\omega)$ are given as

$$a(\omega) = \frac{1}{f(\omega)}\{2a^3\lambda_1(\varepsilon_2^* - \varepsilon_3^*) + b^3[\lambda_1(2\varepsilon_3^* + \varepsilon_2^*) + 3\varepsilon_2^*(\lambda_2 - 3E_0\varepsilon_3^*)]\}, \tag{12}$$

$$b(\omega) = \frac{1}{f(\omega)}\{2a^3\lambda_1(\varepsilon_2^* - \varepsilon_3^*) + b^3[6E_0\varepsilon_3^*(\varepsilon_1^* - \varepsilon_2^*) + 2\lambda_2(\varepsilon_1^* + \varepsilon_2^*)]\}, \tag{13}$$

$$c(\omega) = \frac{1}{f(\omega)}\{a^3b^3[(3E_0\varepsilon_3^* + \lambda_2)(\varepsilon_1^* - \varepsilon_2^*) + \lambda_1(2\varepsilon_3^* + \varepsilon_2^*)]\}, \tag{14}$$

$$d(\omega) = \frac{1}{f(\omega)}\{b^6[E_0(2\varepsilon_2^* + \varepsilon_1^*)(\varepsilon_2^* - \varepsilon_3^*) + 2\lambda_2(\varepsilon_2^* - \varepsilon_1^*)] + a^3b^3[(E_0(2\varepsilon_2^* + \varepsilon_3^*) - \lambda_2)(\varepsilon_1^* - \varepsilon_2^*) + 3\lambda_1\varepsilon_2^*]\}, \tag{15}$$

$$f(\omega) = 2a^3(\varepsilon_1^* - \varepsilon_2^*)(\varepsilon_2^* - \varepsilon_3^*) + b^3(\varepsilon_1^* + 2\varepsilon_2^*)(\varepsilon_2^* + 2\varepsilon_3^*). \tag{16}$$

Here, θ is the polar angle measured by the response to the direction of the external field; ε_1^*, ε_2^* and ε_3^* are complex permittivities corresponding to the interior, membrane and exterior regions in the ICS, respectively. The complex permittivity ε^* is given as

$$\varepsilon^* = \varepsilon + \frac{\sigma}{\mathrm{i}\omega\varepsilon_0}, \tag{17}$$

where ε and σ are the relative permittivity and conductivity, λ_1 and λ_2 are the surface charge densities of the cell and ICS membranes with values of $10^{-3} \sim 10^{-2}$ C/m^2, respectively. In the present work, we choose $\lambda_1 = \lambda_2 = 0.01$ C/m^2. The complex permittivity ε^* can be found in Ref. [28], i.e., $\varepsilon_1^* = \varepsilon_3^* = 80 - 6.8 \times 10^{10}\mathrm{i}/\omega$ and $\varepsilon_2^* = 4$. Set $\varepsilon_2^* = 0$

and $\varepsilon_1^* = \varepsilon_3^* = \varepsilon^*$ for simplicity, then the following relations will be obtained:

$$a(\omega) = \frac{0.01}{\varepsilon^*}, \tag{18}$$

$$b(\omega) = a + \frac{3E_0 b^3}{b^3 - a^3} \quad , \tag{19}$$

$$c(\omega) = \frac{1.5a^3b^3}{b^3 - a^3}(a + E_0), \tag{20}$$

$$d(\omega) = \frac{b^3}{2}\left(\frac{a^4 + 2ab^3}{a^3 - b^3} - E_0\right), \tag{21}$$

where $b(\omega) = b_1$ or b_2 is expressed as

$$b_1 = \frac{a}{\frac{1}{4}(1 - \sqrt{1 + 4y_0}) + \frac{1}{2}\sqrt{\frac{1}{2} - y_0 - \frac{1}{2}\sqrt{1 + 4y_0} + 2\sqrt{y_0^2 - 4}}}, \tag{22}$$

or,

$$b_2 = \frac{a}{\frac{1}{4}(1 - \sqrt{1 + 4y_0}) - \frac{1}{2}\sqrt{\frac{1}{2} - y_0 - \frac{1}{2}\sqrt{1 + 4y_0} + 2\sqrt{y_0^2 - 4}}} \tag{23}$$

with

$$y_0 = \sqrt[3]{\frac{k'^2 + 1}{2} + \sqrt{\frac{(1 + k'^2)^2}{4} + \frac{(k' - 4)^3}{27}}} + \sqrt[3]{\frac{k'^2 + 1}{2} - \sqrt{\frac{(1 + k'^2)^2}{4} + \frac{(k' - 4)^3}{27}}}. \tag{24}$$

Here,

$$k' = 1 + \frac{3E_0}{a}. \tag{25}$$

The radii of the inter and outer ICS membrane are $R_1 = 0.99$ μm and $R_2 = 1$ μm according to Ref. [28], respectively. The transmembrane potential of ICS membrane reads

$$U_{\rm m} = \Phi_3(R_2, \theta) - \Phi_1(R_1, \theta) = \left[\frac{b^3}{2R_2^2}\left(\frac{a^4 + 2ab^3}{a^3 - b^3} - E_0\right) - aR_1 - E_0R_2\right]\cos(\theta). \tag{26}$$

Substituting Eq. (26) into Eq. (8) yields

$$Y = h(\omega, E_0, \theta)X, \tag{27}$$

in which

$$h(\omega, E_0, \theta) = {\rm e}^{\alpha U_0}\left\{1 + \frac{\alpha^2}{4}\left[\frac{b^3}{2R_2^2}\left(\frac{a^4 + 2ab^3}{a^3 - b^3} - E_0\right) - aR_1 - E_0R_2\right]^2\cos^2(\theta)\right\}. \tag{28}$$

Setting $U_0 = 40$ mV, h is a function of ω, E_0 and θ when $b = b_1$ and $b = b_2$ are analysed by numerical calculation, respectively. We find that h appears as a negative value at $b = b_1$ depending on ω and E_0, and that h reaches 10^{20} at $b = b_1$. It is unallowed in physics. Therefore, we take $b = b_2$. The h increases fast as E_0 increases for the case of strong E_0, while h does not vary when E_0 is small. In addition, h varies symmetrically with $\theta = \pi/2$ as θ increases. Substituting Eq. (27) into Eq. (1) yields

$$\frac{{\rm d}X}{{\rm d}t} = A(X) + B\xi(t), \tag{29}$$

in which

$$A(X) = V_0 + V\beta_0 + (hk_{\rm f} - k)X - \frac{V_{1\rm m}X^2}{k_2^2 + X^2} + \frac{V_{2\rm m}h^2X^6}{(k_{\rm a}^4 + X^4)(k_{\rm r}^2 + h^2X^2)}, \tag{30}$$

$$B = VD. \tag{31}$$

This is the LE of the cytosol Ca^{2+} concentration X with an external electromagnetic field. The corresponding FPE is

$$\partial_t P(X, t) = -\partial_X[A(X)P(X, t)] + \frac{1}{2}\partial_X^2[B^2P(X, t)]. \tag{32}$$

The steady-state solution of the FPE is

$$P_{\rm S}(X) = N\left(\frac{X^2-\sqrt{2}k_{\rm a}X+k_{\rm a}^2}{X^2+\sqrt{2}k_{\rm a}X+k_{\rm a}^2}\right)^{-\beta_1}\exp\left\{\beta_2 X+\beta_3 X^2+\beta_4\arctan\left(\frac{X}{k_2}\right)-\beta_5\arctan\left(\frac{hX}{k_{\rm r}}\right)\right.$$
$$\left.-\beta_6\left[\arctan\left(\frac{\sqrt{2}X}{k_{\rm a}}-1\right)+\arctan\left(\frac{\sqrt{2}X}{k_{\rm a}}+1\right)\right]\right\}, \tag{33}$$

where

$$\beta_1=\frac{V_{2{\rm m}}h^2k_{\rm a}^3(k_{\rm r}^2-k_{\rm a}^2h^2)}{2\sqrt{2}V^2D^2(k_{\rm r}^4+k_{\rm a}^4h^4)},\quad \beta_2=\frac{2}{V^2D^2}(V_0-V_{1{\rm m}}+V_{2{\rm m}}+V\beta_0),\quad \beta_3=\frac{hk_{\rm f}-k}{V^2D^2},$$
$$\beta_4=\frac{2k_2V_{1{\rm m}}}{V^2D^2},\quad \beta_5=\frac{2V_{2{\rm m}}k_{\rm r}^5}{hV^2D^2(k_{\rm r}^4+k_{\rm a}^4h^4)},\quad \beta_6=\frac{V_{2{\rm m}}h^2k_{\rm a}^3(k_{\rm r}^2+k_{\rm a}^2h^2)}{\sqrt{2}V^2D^2(k_{\rm r}^4+k_{\rm a}^4h^4)},$$

and N is the normalization constant. In the same way, substituting Eq. (27) into Eq. (33), the SPD of Y can be obtained as

$$P_{\rm S}(Y) = N\left(\frac{Y^2-\sqrt{2}k_{\rm a}hY+k_{\rm a}^2h^2}{Y^2+\sqrt{2}k_{\rm a}hY+k_{\rm a}^2h^2}\right)^{-\beta_1}\exp\left\{\beta_2\frac{Y}{h}+\beta_3\frac{Y^2}{h^2}+\beta_4\arctan\left(\frac{Y}{hk_2}\right)-\beta_5\arctan\left(\frac{Y}{k_{\rm r}}\right)\right.$$
$$\left.-\beta_6\left[\arctan\left(\frac{\sqrt{2}Y}{hk_{\rm a}}-1\right)+\arctan\left(\frac{\sqrt{2}Y}{hk_{\rm a}}+1\right)\right]\right\}. \tag{34}$$

The steady-state mean cytosol and ICS Ca^{2+} concentrations $< X >$ and $< Y >$ are defined as

$$< X >= \int_0^\infty XP_{\rm S}(X){\rm d}X, \tag{35}$$
$$< Y >= \int_0^\infty YP_{\rm S}(Y){\rm d}Y. \tag{36}$$

In the present study, we set $\omega = 1\times10^4{\rm s}^{-1}$ because the SPD of the system and the mean Ca^{2+}concentration do not vary with frequency ω.

3. Results and discussion

In Section 2, we have obtained the expressions of the SPD and the mean Ca^{2+} concentration. Based on these expressions, the effects of the electric field intensity and the polar angle on the SPD $P_{\rm S}(X)$, $P_{\rm S}(Y)$, and the mean $< X >$ and $< Y >$ of the cytosol and the ICS Ca^{2+} concentration can be analysed by numerical calculation method. The results of the numerical calculations are presented in the following figures.

First, we analyse the effects of the electric field intensity and the polar angle on $P_{\rm S}(X)$ and $< X >$. The effects of the polar angle θ on $P_{\rm S}(X)$ are plotted for different electric field intensities (i.e., $E_0 = 1$ V/m and $E_0 = 4.5\times10^3$ V/m) in Fig. 2.

It should be pointed out that the value of θ ranges from 0 to $\pi/2$ because the SPD is symmetrical about $\theta = \pi/2$ in a range between 0 and π. From Fig. 2, one can clearly see that $P_{\rm S}(X)$ cannot be affected by the variation of θ for the case of small E_0, which implies that the polar angle does not affect cytosol calcium oscillation under the condition of weak electric field (see Fig. 2(a)). However, when the electric field is strong, the peak of $P_{\rm S}(X)$ becomes smaller and corresponds to a higher X for the case of smaller θ, which implies that the fluctuation of cytosol calcium strengthens as $\theta \to 0$ or $\theta \to \pi$ (see Fig. 2(b)).

In Fig. 3, $P_{\rm S}(X)$ values with different electric field intensities, i.e., $E_0 = 0.1$ V/m, 2×10^3 V/m, 4×10^3 V/m and 5×10^3 V/m, are plotted for the cases of $\theta = 0$ and $\theta = \pi/2$, respectively. Figure 3 shows that $P_{\rm S}(X)$ has a lower peak with higher X as E_0 increases under the condition of small θ and strong E_0, but $E_0 < 2\times10^3$ V/m does not almost affect SPD, which implies that the fluctuation of cytosol calcium for smaller or larger polar angle increases as strong electric field intensity strengthens (see Fig. 3(a)). But $P_{\rm S}(X)$ cannot be affected by the variation of E_0 for the case of $\theta \to \pi/2$, which implies that the variation of the electric field intensity haw no influence on cytosol calcium oscillation as $\theta \to \pi/2$ (see Fig. 3(b)). The $< X >$ values as a function of electric field intensity for different polar angles are plotted in Fig. 4, which shows that $< X >$ increases as the electric field intensity strengthens when $\theta < \pi/2$ and the speed of its increase decreases with θ increasing, ultimately it remains constant with the electric field intensity increasing when $\theta = \pi/2$.

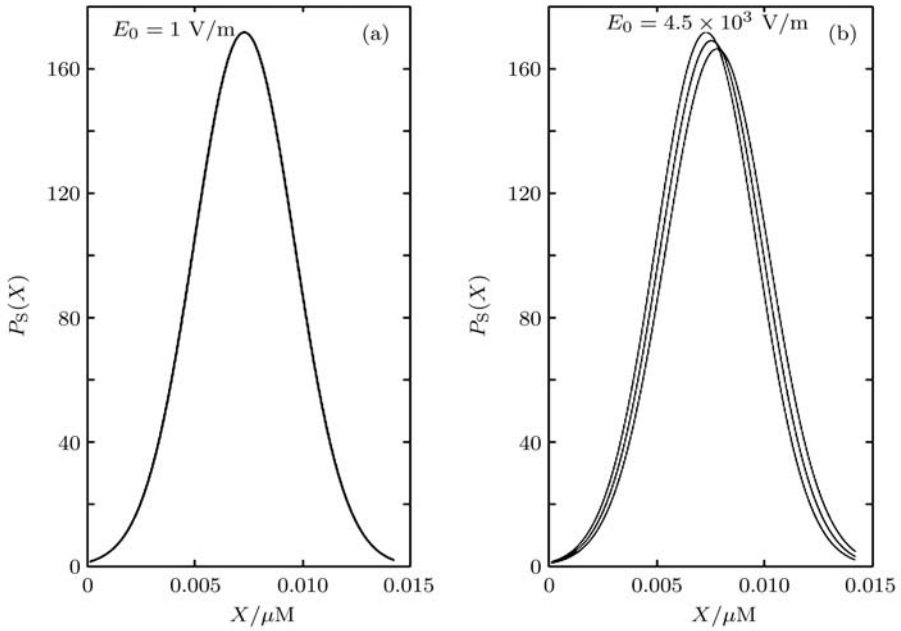


Fig. 2. Plots of steady-state probability distribution $P_S(X)$ versus the cytosol Ca^{2+} concentration X for different values of polar angle θ with (a) $E_0 = 1$ V/m , (b) $E_0 = 4.5 \times 10^3$ V/m, and peaks of $P_S(X)$ from bottom to top corresponding to $\theta = 0$, $\pi/4$ and $\pi/2$ respectively.

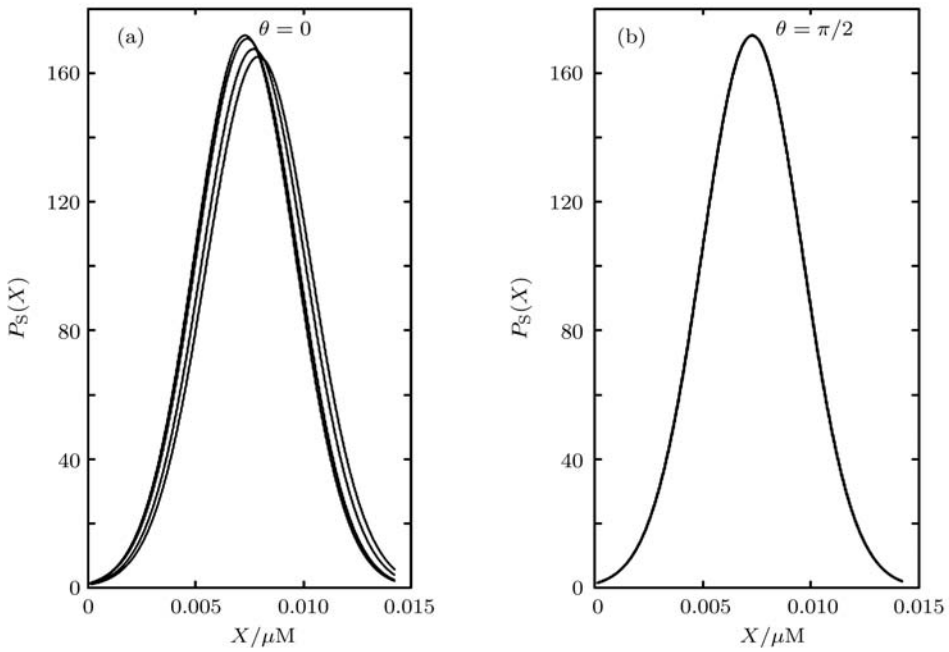


Fig. 3. Plots of steady-state probability distribution $P_S(X)$ versus the cytosol Ca^{2+} concentration X for different values of electric field intensity E_0, with (a) $\theta = 0$, (b) $\theta = \pi/2$, and peaks of $P_S(X)$ from top to bottom corresponding to $E_0 = 0.1$ V/m, 2×10^3 V/m, 4×10^3 V/m and 5×10^3 V/m, respectively.

In Fig. 5, $< X >$ values as a function of the polar angle are plotted for different electric field intensities, i.e., $E_0 = 0.1$ V/m, 2×10^3 V/m, 4×10^3 V/m and 5×10^3 V/m. One can see that as the polar angle increases, $< X >$ decreases for the case of $\theta < \pi/2$ and increases when $\pi/2 < \theta < \pi$, i.e., there is a minimum of $< X >$ at $\theta = \pi/2$. The larger electric field intensity leads to a higher mean cytosol Ca^{2+} concentration. Nevertheless, $< X >$ remains unchanged as θ increases when the electric field intensity is very small (e.g., $E_0 = 0.1$ V/m).

Then, we discuss the effects of electric field intensity and polar angle on $P_S(Y)$ and $< Y >$. When $E_0 = 1$ V/m and $E_0 = 4.5 \times 10^3$ V/m, $P_S(Y)$ values are plotted in Figs. 6(a) and 6(b) for different polar angles ($\theta = 0$, $\pi/4$ and $\pi/2$), respectively.

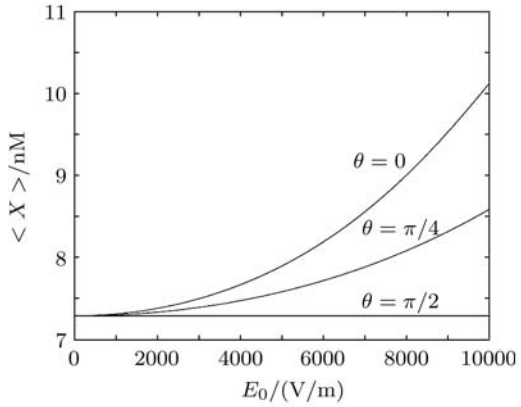


Fig. 4. Plots of the steady-state mean of the Ca^{2+} concentration of cytosol $< X >$ versus electric field intensity E_0 for different values of polar angle θ.

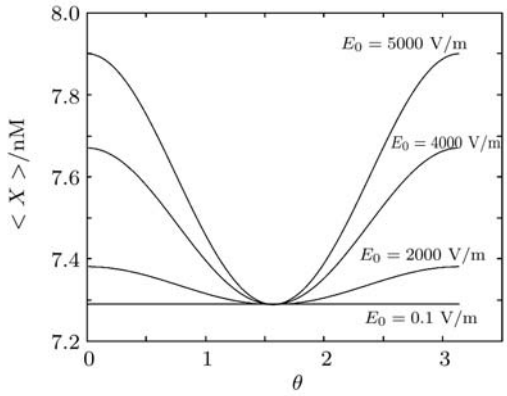


Fig. 5. Plots of the steady-state mean of the Ca^{2+} concentration of cytosol $< X >$ versus polar angle θ for different electric field intensity E_0.

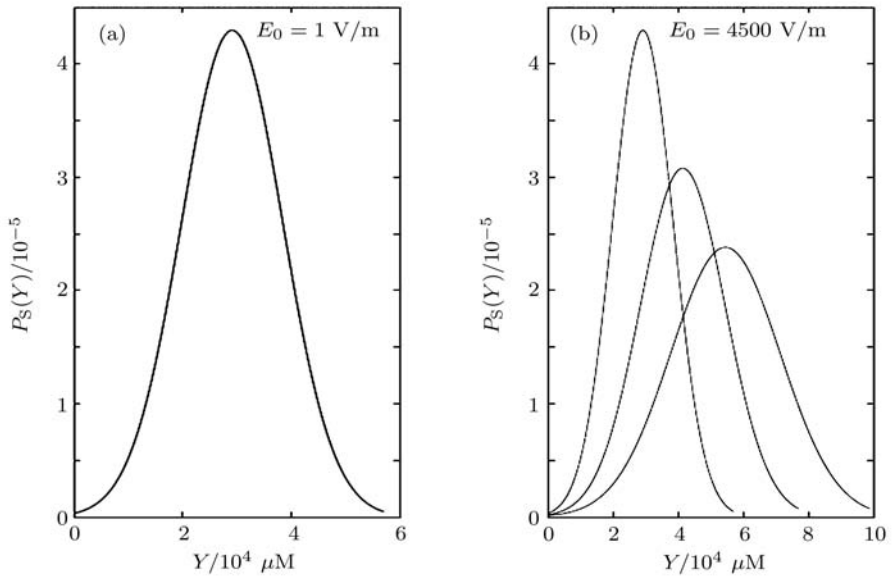


Fig. 6. Plots of steady-state probability distribution $P_S(Y)$ versus Ca^{2+}concentration of ICS Y for different values of polar angle θ with (a) $E_0 = 1$ V/m, (b) $E_0 = 4.5 \times 10^3$ V/m, and peaks of $P_S(Y)$ from bottom to top corresponding to $\theta = 0$, $\pi/4$ and $\pi/2$, respectively.

From Fig. 6, we can see that $P_S(Y)$ is not affected by the variation of θ for the case of small E_0, which shows that the ICS calcium oscillation cannot be affected by the polar angle as the electric field weakens (see Fig. 6(a)). But when the electric field is strong, the peak of $P_S(Y)$ becomes smaller and corresponds to a higher Y as θ descends, which implies that the ICS calcium oscillation strengthens as polar angle θ decreases or increases (see Fig. 6(b)). The effects of the electric field intensity on $P_S(Y)$ are shown in Figs. 7(a) and 7(b) for $\theta = 0$ and $\pi/2$, in which for each θ we take $E_0 = 0.1$ V/m, 2×10^3 V/m, 4×10^3 V/m and 5×10^3 V/m.

From Fig. 7, one can see that $P_S(Y)$ has a lower peak with higher Y as E_0 increases under the the condition of small θ and strong E_0, which implies that the ICS calcium oscillation strengthens with the electric field intensity increasing when the polar angle is small or large (see Fig. 7(a)). But $P_S(Y)$ cannot be affected by the variation of E_0 for the case of$\theta \to \pi/2$, which manifests that the ICS calcium oscillation cannot be modified by the electric field intensity when $\theta = \pi/2$ (see Fig. 7(b)). The curves for $< Y >$ versus electric field intensity are plotted in Fig. 8 for different polar angles: $\theta = 0$, $\pi/4$ and $\pi/2$. The $< Y >$ first increases and then decreases as the electric field intensity strengthens, and its peak position shifts towards the larger values of the electric field intensity with polar angle increasing, but it keeps constant when $\theta = \pi/2$. The variations of $< Y >$ with polar angle are plotted in Fig. 9 for different electric field intensities: $E_0 = 0.1$ V/m, 2×10^3 V/m, 4×10^3 V/m, and 5×10^3 V/m.

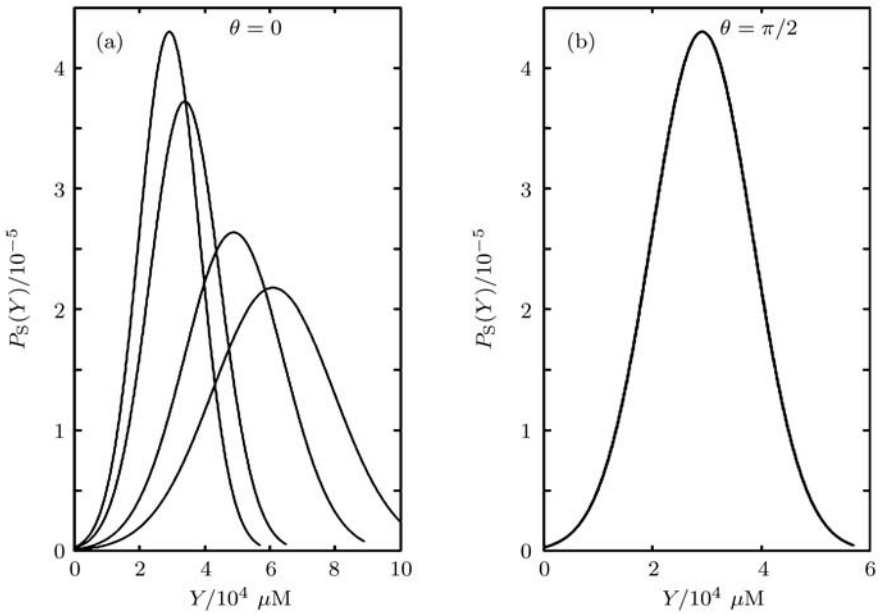


Fig. 7. Plots of steady-state probability distribution $P_S(Y)$ versus Ca^{2+}concentration of ICS Y for different values of electric field intensity E_0, with (a) $\theta = 0$, (b) $\theta = \pi/2$, and peaks of $P_S(Y)$ from top to bottom corresponding to $E_0 = 0.1$ V/m, 2×10^3 V/m, 4×10^3 V/m and 5×10^3 V/m, respectively.

Figure 9 indicates that $< Y >$ goes down as the polar angle increases when $\theta < \pi/2$ and goes up in a range of $\pi/2 < \theta < \pi$, and the larger the electric field intensity is, the higher the mean Ca^{2+} concentration of the ICS is, except in the cases where the electric field intensity is small.

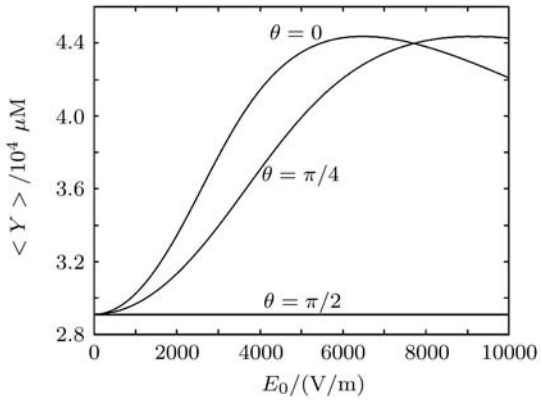


Fig. 8. Plots of steady-state mean of the Ca^{2+} concentration of ICS $< Y >$ versus electric field intensity E_0 for different values of polar angle θ.

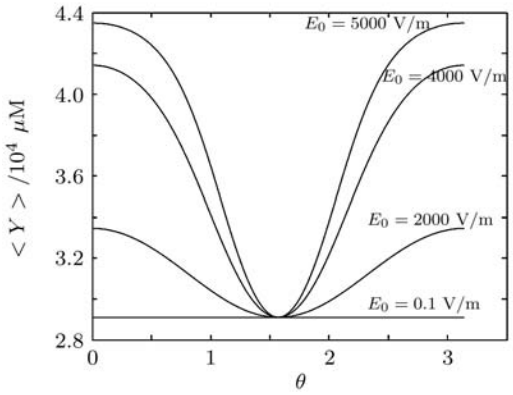


Fig. 9. Plots of steady-state mean of the Ca^{2+} concentration of ICS $< Y >$ versus polar angle θ for different electric field intensity E_0.

4. Conclusion

We have investigated intracellular calcium ion concentration oscillation in a cell subjected to external noise and irradiated by an electromagnetic field. The results indicate that in a cell irradiated by an external electromagnetic field, being in a stationary state, under the condition of appropriate external noise intensity, the frequency of the electromagnetic field generally has no influence on the cytosol and ICS calcium oscillation. In the case of a small electric field intensity or the polar angle $\theta \to \pi/2$, the cytosol and ICS calcium oscillations cannot be affected by the external electromagnetic field. When the electric field intensity is large and the polar angle is small ($\theta \to 0$) or large ($\theta \to \pi$), the cytosol and ICS calcium oscillations are strengthened by the external electromagnetic field. Therefore, the calcium oscillation of the cytosol is synchronous with the ICS of a cell in the electromagnetic field. For the weak electric field intensity or the polar angle $\theta \to \pi/2$, the steady-state mean Ca^{2+} concentration of cytosol and the ICS are not af-

fected by the external electromagnetic field. For the cases of the large electric field intensity and the small or large polar angle, the steady-state mean Ca^{2+} concentration of cytosol and the ICS rise as electric field intensity increases and, as polar angle increases, it first descends and then increases. Therefore, the change of Ca^{2+} concentration of cytosol is synchronous with the ICS when the cell is in electromagnetic field.

References

[1] Berridge M J, Bootman M D and Lipp P 1998 *Nature* **395** 645

[2] Dupont G, Goldbeter A and Berridge M J 1990 *Cell Regul.* **1** 853

[3] Falcke M, Or-Guil M and Bär M 2000 *Phys. Rev. Lett.* **84** 4753

[4] Sakaguchi H and Woafo P 2008 *Phys. Rev.* E **77** 042902

[5] Houart G, Dupont G and Goldbeter A 1999 *Bull. Math. Biol.* **61** 507

[6] Jafri M S, Vajda S, Pasik P and Gillo B 1992 *Biophys. J.* **63** 235

[7] Eichwald C and Kaiser F 1993 *Biophys. J.* **65** 2047

[8] Reidl J, Borowski P, Sensse A, Starke J, Zapotocky M and Eiswirth M 2006 *Biophys. J.* **90** 1147

[9] Höfer T 1999 *Biophys. J.* **77** 1244

[10] Lavrentovich M and Hemkin S 2008 *J. Theor. Biol.* **251** 553

[11] Hallén K, Huss M, Kettunen P, Manira A E and Kotaleski J H 2004 *Neurocomputing* **58-60** 431

[12] Atri A, Amundson J, Clapham D and Sneyd J 1993 *Biophys. J.* **65** 1727

[13] Somogyi R and Stucki J W 1991 *J. Biol. Chem.* **266** 11068

[14] Tesarik J and Sousa M 1996 *Molecular Human Reproduction* **2** 383

[15] Kraus M, Wolf B and Wolf B 1996 *Cell Calcium* **19** 461

[16] Berridge M J 1994 *Biochem. J.* **302** 545

[17] Gapeyev A B and Chemeris N K 1999 *J. Biol. Phys.* **25** 193

[18] Zhong S, Qi F and Xin H 2001 *Chem. Phys. Lett.* **342** 583

[19] Li Q S and Wang P 2004 *Chem. Phys. Lett.* **387** 383

[20] Li H, Hou Z and Xin H 2005 *Phys. Rev.* E **71** 061916

[21] Yu G, Yi M, Jia Y and Tang J 2009 *Chaos, Solitons and Fractals* **41** 273

[22] Li Q and Wang Y 2007 *Biophys. Chem.* **129** 23

[23] Li H, Hou Z and Xin H 2005 *Chem. Phys. Lett.* **402** 444

[24] Läer L, Kloppstech M, Schöfl C, Sejnowski T J, Brabant G and Prank K 2001 *Biophys. Chem.* **91** 157

[25] Kusters J M A M, Cortes J M, Meerwijk W P M V, Ypey D L, Theuvenet A P R and Gielen C C A M 2007 *Phys. Rev. Lett.* **98** 098107

[26] Li Y P and Li Q S 2004 *Chem. Phys. Lett.* **392** 95

[27] Li Q X and Niu Z Q 1990 *Introduction to Bioelectromagnetics* (Vol.1) (Xian: Xian Electronics Science and Technology University Press) pp278–284 (in Chinese)

[28] Joshi R P, Hu Q, Schoenbach K H and Beebe S J 2004 *Phys. Rev.* E **69** 051901

[29] Vajrala V, Claycomb J R, Sanabria H and Millera J H 2008 *Biophys. J.* **94** 2043